Silicon (2018) 10:2653–2662
https://doi.org/10.1007/s12633-018-9802-7

ORIGINAL PAPER

Synthesis, Characterization and Wire Electric Erosion Behaviour of AA7178-10 wt.% ZrB_2 Composite

S. Dinesh Kumar[1] **· M. Ravichandran**[2]

Received: 19 July 2017 / Accepted: 7 March 2018 / Published online: 16 April 2018

Abstract

In this work, AA7178-10 wt.% ZrB_2 Metal Matrix Composite was produced using stir casting route and the mechanical properties of the composites were studied. The microstructure and elemental verification were done by using Scanning Electron Microscope (SEM) and Energy Dispersive X-Ray Spectroscopy (EDS). Among the various non-traditional machining processes, Wire Electrical Discharge Machining (WEDM) is an important process for machining MMCs. The objective of this work is to investigate the effect of Peak current (I), Pulse On-Time (PT_{On}), Pulse Off Time (PT_{Off}) and Wire feed rate (WF) on the combined objective of maximum Metal Removal Rate (MRR) and minimum Surface Roughness (SR) during machining of AA7178-10 wt.% ZrB_2 composite using Taguchi based Grey Relational Analysis (GRA). L_{16} orthogonal array, for the four machining parameters at four levels each, was opted to conduct the experiments. Analysis of variance (ANOVA) was performed to find the validity of the experimental plan followed in the present work. Results show that, maximum MRR and minimum SR can be achieved for the peak current (11 A), Pulse On-Time (112 µs), Pulse Off Time (45 µs) and Wire feed rate (7 m/min).

Keywords AA7178 · ZrB_2 · Stir casting · Composites · Taguchi grey relational analysis · WEDM

1 Introduction

Metal Matrix composites (MMC's) have high strength, high stiffness, damping resistance, high wear resistance, light weight, very good elevated temperature properties, impact as well as good shock absorption, good dimensional stability and castability [1, 2]. MMCs have great potential for aerospace, automobile and other applications because of their good properties [3, 4]. Further these composites are of superior in nature for elevated temperature application when reinforced with ceramic particles [5, 6]. The type of reinforcement material has a considerable effect on the mechanical and structural properties of the composites [7]. Zirconium diboride (ZrB_2) is an ultra high temperature ceramic that has strong covalent bonding, which gives it a melting temperature of 3250 °C, high hardness of 23 GPa, and high elastic modulus of 546 GPa. The bonding also has metallic character, which results in high thermal conductivity (60 W/m K) and electrical conductivity (107 S/m). With this exceptional properties, ZrB_2 shows promise for diverse applications such as cutting tools, molten metal crucibles, thermal protection systems for hypersonic aerospace vehicles, and which makes it attractive for aerospace applications [8, 9]. To improve the mechanical properties of MMCs, many researchers have prepared composites by ex situ method. Many researchers fabricated zircon reinforced MMCs using different techniques and reported their microstructure and mechanical properties [10]. Many methods have been used for fabrication of Al matrix composites such as, infiltration, squeeze casting, mechanical alloying, powder metallurgy, ball milling, and stir casting [11]. The processing method influences the mechanical behavior of the AMCs because of the successful incorporation of ceramic particles into the matrix alloy is important to achieve good properties [12]. The particulate reinforced composite can be prepared by introducing the reinforcing particles into liquid matrix through liquid metallurgy route by casting. Casting route is preferred as it is less expensive and suitable for mass production [13,

✉ M. Ravichandran
smravichandran@hotmail.com

1 Department of Mechanical Engineering, Chendhuran College of Engineering and Technology, Pudukkottai, 622 507, Tamil Nadu, India

2 Department of Mechanical Engineering, Chennai Institute of Technology, Chennai, 600 069, Tamil Nadu, India

14]. Some important advantages of casting route are: better matrix-particle bonding, easier control of matrix structure, simplicity, low cost of processing and nearer net shape and the wide selection of materials for this fabrication method [15]. Metal matrix composites reinforced with hard ceramic fibers, particles can be machined with either an electroplated diamond grinding wheel or carbide with poly crystalline diamond cutting tools. As a consequence, non-conventional machining process like electro discharge machining (EDM), laser and other Wire EDM were increasingly being applied for the machining of particle reinforced metal matrix composites [16]. WEDM has been quite successful for machining of MMCs and its process parameters greatly influences the MRR, SR, corrosion behaviour and fatigue strength [17]. This process is widely applied not only in tool and die-making industry, but also in the fields of production of parts for medicine, electronics, and the automotive industry [18]. In WEDM Process, wire electrode and work piece never make contact therefore, there is virtually no cutting force on the part, thus it is free from mechanical stresses [19]. Recently, WEDM process is also being used to machine a wide variety of miniature and micro-parts in metals, alloys, sintered materials, cemented carbides, ceramics and silicon [20]. Garg et al. reported the theoretical models for simulating the input and output parameters for MMCs on EDM processes [21]. Ashwani Kharola revealed the effects of discharge current on various machining output parameters of Die-Sinking EDM including MRR, TWR and SR for different hard materials [22]. Cheng Wang et al. reported MRR increased with peak current and pulse duration and this is due to more discharge energy delivered to the machining zone to promote thermal erosion effects such as melting, vaporization, and thermal spalling during the EDM process [23]. Suresh Kumar et al. have done the experimental work in machining of aluminium based composites and reported that the surface roughness increases for the increase in pulse duration [24].

Taguchi method can be utilized to determine the optimal machining parameters in a WEDM process. From the basic principle and characteristic feature of the WEDM process for the machining of composites and it has been observed that the machining parameters, such as pulse on-time (TON), pulse off-time (TOFF), peak current (IP) wire feed rate (WF), are the important controllable process parameters of the WEDM process [25]. The GRA based on grey system theory can be used for solving the complicated interrelationships among the multi responses [26, 27]. The integrated grey based Taguchi method combines advantages of both Taguchi method and GRA. Furthermore, ANOVA can be performed to see which process parameters are statistically significant [28]. Muthuramalingam and Mohan used the GRA for the determination of optimal EDM Parameters with the objective of minimization of SR [29]. Rajesh kannan et al. used the grey relational analysis method for optimization of the electric discharge drilling parameters with the objective of minimization of SR [30].

In this investigation, the WEDM process parameter such as Pulse on time (µs), Pulse off time (µs), Wire feed rate (m/min) and Peak Current (A) were optimized for the responses such as MRR and SR for machining stir cast AA7178 – 10 wt. % ZrB_2 composites. The Taguchi L16 orthogonal array has been used to conduct the experiments. The Analysis of variance (ANOVA) was used to obtain the total percentage of contribution of each parameter for MRR and SR. Taguchi based GRA was used o identify the parameters for combined objective of maximum MRR and minimum SR.

2 Materials and Methods

In this investigation, Aluminium 7178 was considered as matrix material and ZrB_2 particles were used as reinforcement. The AA7178 contains alloying elements such as Si: 0.4, Fe: 0.5, Cu: 1.8, Mg: 2.5, Mn: 0.3, Cr: 0.28, Zn: 7.1, Ti: 0.2 and remaining Al in weight percentages. The reason for selecting this material is that, generally the AA7xxx alloys have been widely used in aircraft and automobile applications because of their high strength and low weight [31]. The 7178 series alloys based on Al–Zn–Mg system have unique combination of desirable characteristics including low density, high strength and fracture toughness [32]. The SEM image of as received ZrB_2 particles is shown in Fig. 1 and it ensures the particles size is less than 10 µm. Figure 2 shows the XRD pattern of ZrB_2 powders and it evident the presence of Zr and B phases and the absence of other phases and also the respective planes are noted in the XRD image. The known quantities of ZrB_2 were added into the molten AA7178 alloy to produce AA7178-10 wt. % ZrB_2 composite using stir casting route. The reason for selecting 10wt. % of ZrB_2 is that, Asadipanah and Rajabi suggested after conducting all mechanical testing that the optimum amount of ZrB_2 reinforcement for fabricating the AMC is to be 10% and reported that the inclusion of more reinforcements in the matrix lead to particles clustering [33]. The temperature of the molten AA7178 was maintained at 850 °C and stirred for 40 min. The composite melt was poured into a preheated die after the removal of slag. Specimens were prepared from the castings to carry out microstructure. The specimens were polished using standard metallographic technique and etched with Keller's reagent for microstructure analysis using SEM.

The WEDM process was conducted for the AA7178-10%ZrB_2 composite using ECOCUT WEDM machine. The four input process parameters namely peak current, pulse on time, pulse off time) and wire feed rate were chosen as

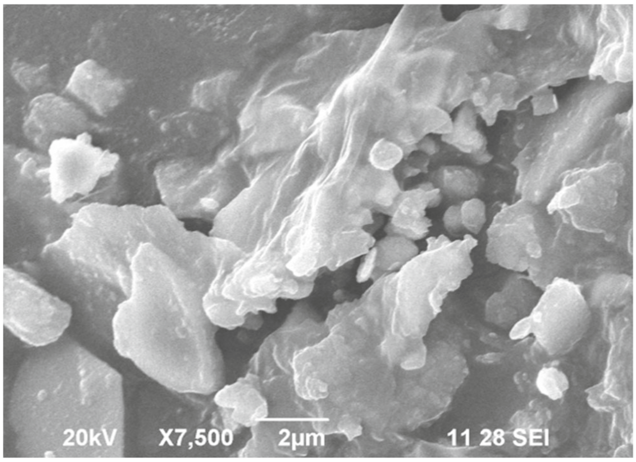

Fig. 1 SEM image of ZrB_2 powder

variables to study their effects on MRR and SR as response parameter. The ranges of input parameters were selected on the basis of literature survey, machine capability and conducting preliminary experiments as shown in Table 1. The machining was carried out as per L_{16} orthogonal array as shown in Table 2 to cut the specimen of Dimension 8× 8× 30 mm in the work material. The machining performance criteria selected for this study were based on performance characteristics such as MRR and SR. Material removal rate has been calculated by weight difference of workpiece before and after the machining process using the formula, MRR=(Wa-Wb)/t, where Wa and Wb are weights of the work piece before and after machining, and 't' is the machining time in minutes. The surface roughness measurements for the machined surface were performed using Mitutoyo surftest SJ-210. The responses obtained for all the experiments are provided in Table 2.

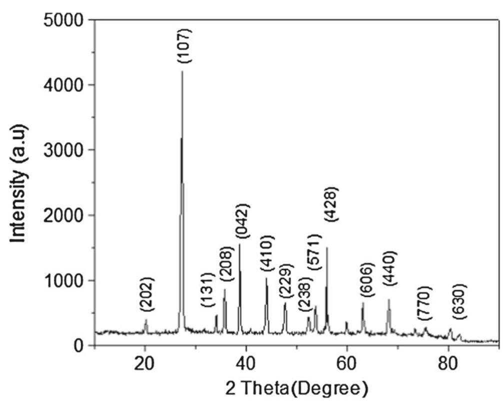

Fig. 2 XRD analysis of ZrB_2 powder

Table 1 Control Factors and Levels

Parameters	Levels			
	1	2	3	4
Pulse on time (µs)	108	110	112	114
Pulse off time (µs)	45	50	55	60
Wire feed (m/min)	1	4	7	10
Current (A)	5	7	9	11

3 Result and Discussion

3.1 SEM Analysis of AA7178 - 10% wt. ZrB_2 Composites

SEM images of AA7178 and AA7178 - 10% wt. ZrB_2 composites are shown in Fig. 3a–c. Figure 3a shows the SEM image of AA7178 and ensures the absence of reinforcement particles. From 3(b) and 3(c) shows the microstructure of AA7178 - 10% wt. ZrB_2 composites fabricated by using stir casting method. The presence of ZrB_2 particles in the composite is evident and the distribution of ZrB_2 particles in the AA7178 matrix is uniform. Figure 3c shows the microstructure of AA7178 - 10% wt. ZrB_2 composites at 50 µm scale and it shows the distribution of the ZrB_2 in the grain boundary of the composite. This result ensures the produced composite has good microstructure and the stir casting route is the right choice for producing AA7178 - 10% wt. ZrB_2 composites. The black flakes are also observed in Fig. 3c which could be the intermetallic formed due to the melting process. The presence alloying elements such as Zn, Mg and Cu forms finer inter-metallic precipitates during melting process [32, 33].

3.2 Multi Response S/N Ratio for MRR and SR

Taguchi Method is systematic and efficiency approach to find the optimal combination of input parameters. This method utilizes the orthogonal array of experiments to reduce the number of experiments and L16 orthogonal array has been selected for the present studies. During WEDM of AA7178 - 10% wt. ZrB_2 composites, two categories of performance characteristics has been considered for analyzing S/N ratio, since we require maximum MRR and minimum SR, the larger the better and smaller the better characteristic was selected according to the required output characteristics. S/N ratio was calculated for minimization quality characteristics and maximization quality characteristics of output responses are reported elsewhere. Therefore, the MRR is regarded as a "larger-the-better" characteristics by using Eq. 1 [26] and for the SR "smaller-the-better" characteristics by using Eq. 2 [26].

Table 2 Experimental layout as per L16 OA

Experiment number	T_{on} (μs)	T_{off} (μs)	WF (m/min)	I (A)	Responses	
					MRR (g/min)	SR (μm)
1	108	45	1	5	0.028	1.533
2	108	50	4	7	0.170	2.717
3	108	55	7	9	0.080	3.245
4	108	60	10	11	0.108	2.744
5	110	45	4	9	0.034	2.523
6	110	50	1	11	0.181	3.482
7	110	55	10	5	0.160	3.239
8	110	60	7	7	0.129	2.145
9	112	45	7	11	0.170	1.859
10	112	50	10	9	0.077	2.328
11	112	55	1	7	0.136	3.123
12	112	60	4	5	0.024	1.801
13	114	45	10	7	0.054	1.924
14	114	50	7	5	0.104	3.652
15	114	55	4	11	0.136	3.567
16	114	60	1	9	0.068	3.733

Thus the S/N ratio is given by:

Larger - the – better

$$\frac{S}{N}\text{ratio}\,(\eta) = -10\log_{10}\left(\frac{1}{n}\right)\sum_{i=1}^{n}\frac{1}{y_{ij}^{2}} \tag{1}$$

where n = number of replications

y_{ij} =observed response value

i = 1, 2, ...n

j = 1, 2...k

This is applied for problem where maximization of the quality characteristic of interest is sought. This is referred as the larger-the-better type problem.

Smaller - the - better

This is termed as the smaller – the - better type problem where minimization of the characteristic is intended.

$$\frac{S}{N}\text{ratio}\,(\eta) = -10\log_{10}\left(\frac{1}{n}\sum_{i=1}^{n}y_{ij}^{2}\right) \tag{2}$$

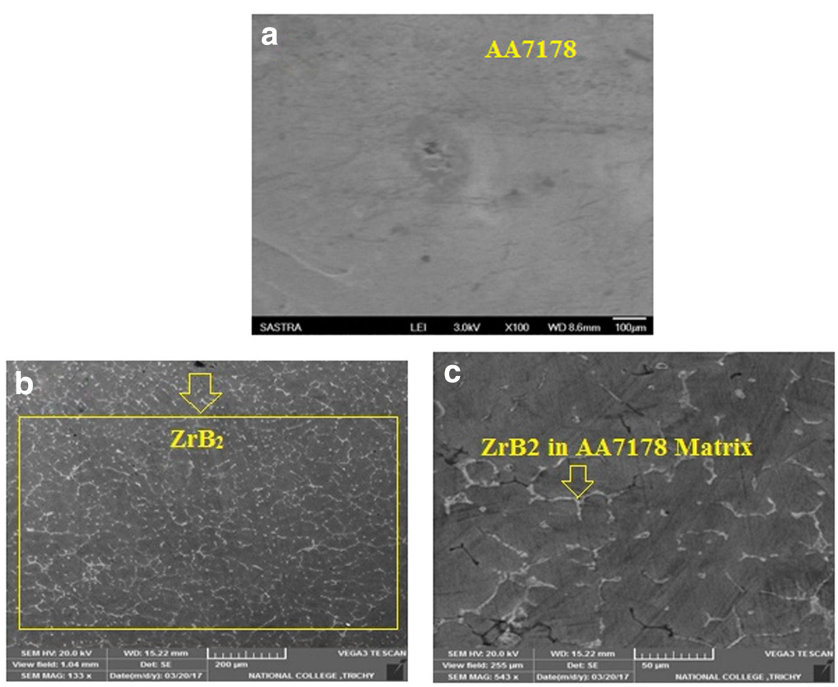

Fig. 3 SEM images of **a** AA7178 **b** & **c** AA7178-10%wt.ZrB_2 composite

Table 3 S/N ratio values and normalized S/N ratio values

Exp. no.	S/N ratio		Normalized S/N ratio	
	MRR	SR	MRR	SR
1	−31.0568	−3.71084	0.025478	1
2	−15.391	−8.68179	0.929936	0.461818
3	−21.9382	−10.2243	0.356688	0.221818
4	−19.3315	−8.76768	0.535032	0.449545
5	−29.3704	−8.03835	0.063694	0.55
6	−14.8464	−10.8366	1	0.114091
7	−15.9176	−10.2082	0.866242	0.224545
8	−17.7882	−6.62855	0.66879	0.721818
9	−15.391	−5.38559	0.929936	0.851818
10	−22.2702	−7.33966	0.33758	0.638636
11	−17.3292	−9.89144	0.713376	0.277273
12	−32.3958	−5.11027	0	0.878182
13	−25.3521	−5.6841	0.191083	0.822273
14	−19.6593	−11.2506	0.509554	0.036818
15	−17.3292	−11.0461	0.713376	0.075455
16	−23.3498	−11.4412	0.280255	0

3.3 Grey Relational Analysis

The grey relational analysis is a multi objective optimization process used to determine the optimum combination of the input parameters and also to determine the influence of each machining parameter on the machining characteristics.

The values should be normalized before being analyzed with the grey relation theory. Here, the experimental result for the responses was normalized and was rated between 0 and 1. The normalized output parameters corresponding to the smaller the better and larger the better criterion can be calculated using Eqs. 3 and 4 [26]. The calculated S/N ratio values and normalized S/N ratio values for the MRR and SR are presented in Table 3.

$$Z_{ij} = \frac{y_{ij-\min}\left(y_{ij,i=1,2,....n}\right)}{\max\left(y_{ij,i=1,2,.....n}\right) - \min\left(y_{ij,i=1,2,....n}\right)} \quad (3)$$

(To be used for S/N ratio with Larger the better manner)

$$Z_{ij} = \frac{max\left(y_{ij,i=1,2,....n}\right) - y_{ij}}{\max\left(y_{ij,i=1,2,.....n}\right) - \min\left(y_{ij,i=1,2,....n}\right)} \quad (4)$$

(To be used for S/N ratio with smaller the better manner)

y_{ij} is normalized as Zij ($0 \leq Z_{ij} \leq 1$) by the following formula to avoid the effect of adopting different units and to reduce the variability. It is necessary to normalize the original data before analyzing them with the grey relation theory. An appropriate value is deducted from the values in the same array to make the value of this array approximate to 1. Since the process of normalization affects the rank, we also analyzed the sensitivity of the normalization process on the sequencing results. Thus, we recommend that the S/N ratio value be adopted when normalizing data in GRA.

The grey relational co-efficient for the normalized S/N ratio values can be determined by using Eq. 5 [26].

$$\gamma(y_0(k), y_1(k)) = \frac{\Delta\min + \xi\Delta\max}{\Delta_{oj}(k) + \xi\Delta\max} \quad (5)$$

Table 4 Deviation Sequence, Grey Relational Coefficient and Grey Relational Grade

Exp. no.	Deviation sequence		Grey relational coefficient		Grey relational grade	Rank
	MRR	SR	MRR	SR		
1	0.974522	0	0.339093	1	0.669546	4
2	0.070064	0.538182	0.877095	0.481611	0.679353	3
3	0.643312	0.778182	0.437326	0.391181	0.414253	15
4	0.464968	0.550455	0.518152	0.475984	0.497068	11
5	0.936306	0.45000	0.348115	0.526316	0.437216	13
6	0	0.885909	1	0.360774	0.680387	2
7	0.133758	0.775455	0.788945	0.392017	0.590481	6
8	0.33121	0.278182	0.601533	0.642523	0.622028	5
9	0.070064	0.148182	0.877095	0.771388	0.824242	1
10	0.66242	0.361364	0.430137	0.580475	0.505306	10
11	0.286624	0.722727	0.635628	0.408922	0.522275	9
12	1	0.121818	0.333333	0.804094	0.568713	7
13	0.808917	0.177727	0.381995	0.73776	0.559878	8
14	0.490446	0.963182	0.504823	0.341721	0.423272	14
15	0.286624	0.924545	0.635628	0.350989	0.493308	12
16	0.719745	1	0.409922	0.333333	0.371628	16

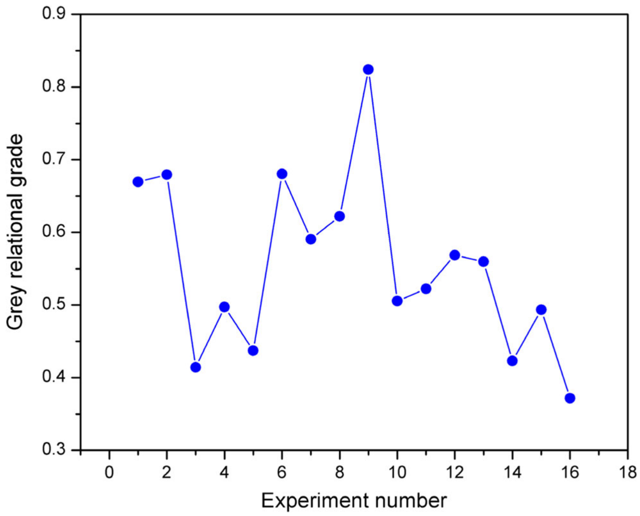

Fig. 4 Time Series Plot of Grey relational grade

Where,

a. j = 1,2…n; k = 1,2…m, n is the number of experimental data items and m is the number of responses.
b. $y_o(k)$ is the reference sequence ($y_o(k)$ = 1, k = 1,2…m); $y_j(k)$ is the specific comparison sequence.
c. $\Delta_{oj} = \left\| y_0(k) - y_j(k) \right\|$ = The absolute value of the difference between $y_o(k)$ and $y_j(k)$
d. $\Delta \min = \min_{\forall j \in i} \min_{\forall k} \left\| y_0(k) - y_j(k) \right\|$ is the smaller value of $y_j(k)$
e. $\Delta \max = \max_{\forall j \in i} \max_{\forall k} \left\| y_0(k) - y_j(k) \right\|$ is the largest value of $y_j(k)$
f. ξ is the distinguishing coefficient which is defined in the range $0 \leq \xi \leq 1$ (the value may be adjusted based on the practical needs of the system)

The grey relational Coefficient is used for calculating the grey rational grade for combined objectives and is ranked in order. The performance standard is evaluated based on this and it is calculated using Eq. 6 [26].

$$\overline{\gamma} = \frac{1}{k} \sum_{i=1}^{m} \gamma_{ij} \tag{6}$$

where γ_j is the grey relational grade for the j_{th} experiment and k is the number of performance characteristics. The calculated grey relational coefficient and Grey relational grade are provided in Table 4. It was observed from Table 4 that the experiment number 9 exhibits the highest grey relational grade. Figure 4 shows the grey relational grade versus experiment number and it shows that the experiment number 9 has high grey relational grade (0.8242), which consists of a better combination of optimal parameter (Ton= 112 µs, Toff = 45 µs, Wire feed = 7 m/min and I = 11 A) with an objective to minimize the SR and maximize the MRR.

3.4 Analysis of Means and SN Ratios

Analysis of the means was performed for the obtained grey relational grade based on the difference between the highest and the lowest average of grey relational grade. From Fig. 5, it is observed that the parameter levels of 3, 1, 3 and 4 have higher grey relational grade which consist of a better combination of optimal parameter level ($A_3B_1C_3D_4$). The increase of pulse duration causes higher discharge energy and also increase in discharge current causes increase of discharge energy which affects SR by increasing in diameter and depth of the discharge craters. Peak current and pulse on period are the most significant and influencing machining parameters for controlling the MRR and SR [24]. Figure 6

Fig. 5 Main effect plot for means

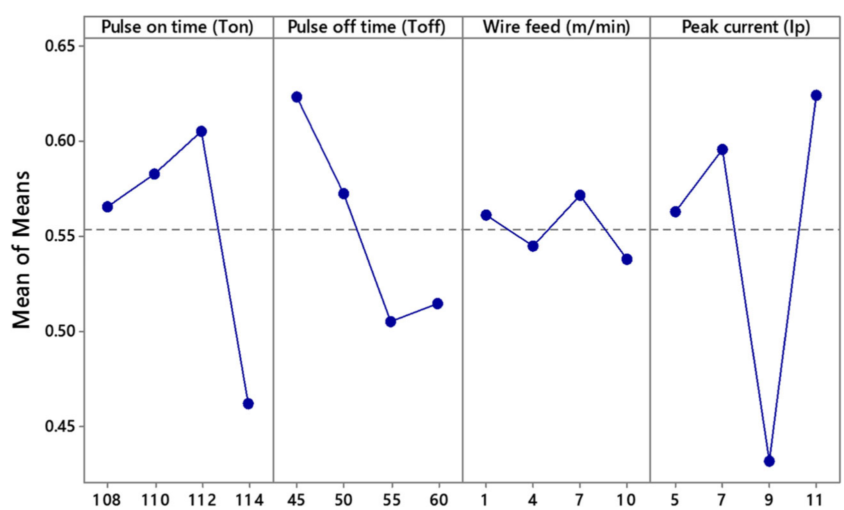

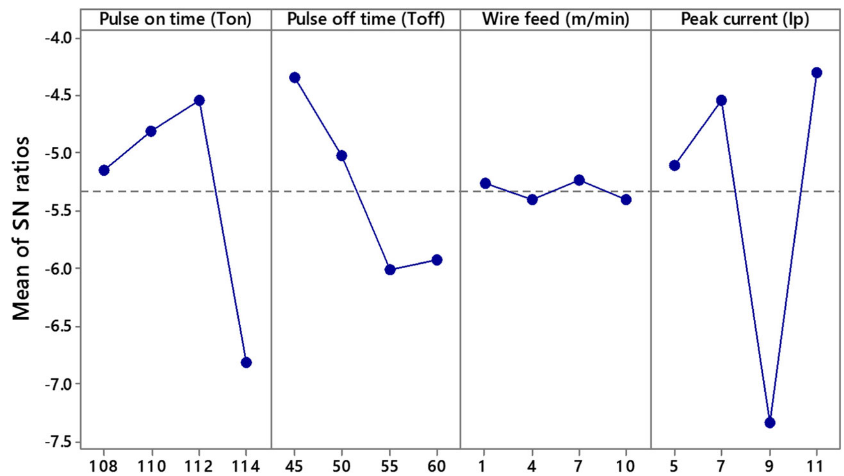

Fig. 6 Main effect plot for SN ratios

shows the main effect plot for Signal to Noise Ratios and the results obtained for analysis of mean and analysis of SN ratio are similar. This ensures the experimental data taken during the machining process is correct.

3.5 Interaction of Parameters with Grey Relational Grade

Figure 7 shows the interaction plot of Grey relational grade for combined objective of SR and MRR during WEDM of AA7178-10 wt. % ZrB_2 composite. The interactions of all the four input factors were studied using this plot. The parallel lines denote the insignificance and unparallel lines denotes significant presence of interaction effect of parameters on the response. In the present study, the interaction of peak current with wire feed rate shows the peak current is the dominate factor for MRR and SR of the composite and it is evident from the non parallel lines of interaction plot. This is due to the high amount of current will produce the high amount of thermal energy and thus the material removal is achieved. Also the discharge energy increases with the pulse on time and peak current leading to a faster machining of composites. Since the pulse off time decreases, the number of discharges increases thus a higher cutting rate is achieved. While interact pulse off time, pulse on time with current, the current is the dominant factor next to the pulse on time. The reason is that, the increase in both pulse on time and current will lead to increase in thermal energy and that will enhance the vaporization of the material. These results are well agreed with the previous findings by various researchers who reported for the different composite materials [26–28, 34]. The interaction of pulse on time with wire feed rate shows that the pulse on time is the most dominant factor and the interaction of pulse off time with wire feed rate also results the same. The reason is that when compare pulse on time and pulse off time with

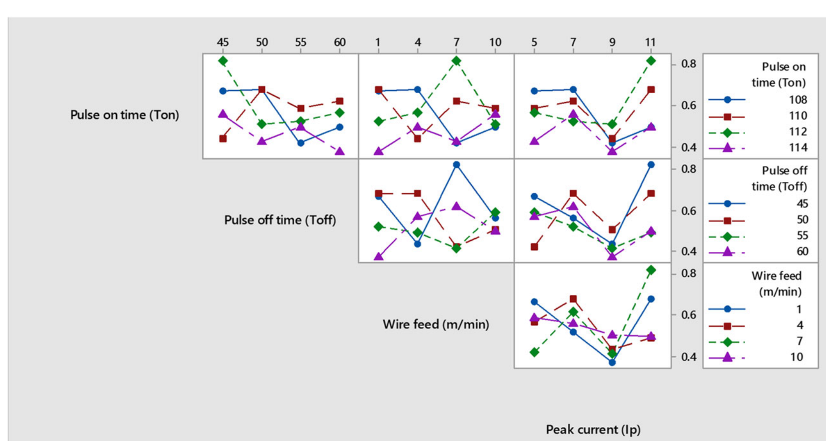

Fig. 7 Interaction plot for Grey relational grade

wire feed rate these two factors are responsible to produce thermal energy and the developed energy is responsible for material removal during machining.

3.6 ANOVA Analysis

ANOVA is the statistical tool and which is applied to confirm the impact of all factors and their interactions by finding out the difference between the mean square and experimental errors at specific confident levels. In this work, ANOVA was performed to find out the significant factors and insignificant factors. The results obtained from ANOVA analysis are shown in Table 5. It can be concluded that the significant factor affecting the grey relational grade is Peak current (39.54%) influences more on machining of AA7178-10 wt. % ZrB_2 MMC followed by Pulse on time (22.02%), Pulse off time (16.46%) and Wire feed (1.23%). The wire feed rate was identified as insignificant factor during machining of AA7178-10 wt. % ZrB_2 MMC. The increase in current value increases the both MRR and SR. The reason is that the increase in current increases the heat generation and thus the increase in erosion is occurred during machining. In general more removal of material during machining will affect the surface finish of the part to be machined. In this study, the most dominant factor is current and pulse on time to machine the MMCs.

3.7 Determine the Optimal Factor and its Level Combination

The higher grey relational grade implies the better product quality; therefore, on the basis of grey relational grade, the factor effect can be estimated and the optimal level for each controllable factor can also be determined.

For example, to estimate the effect of factor i, we calculate the average of grade values (AGV) for each level j, denoted as AGV_{ij}, then the effect, E_i, is defined as:

$$E_{\mathrm{i}} = \max(AGV_{\mathrm{ij}}) - \min(AGV_{\mathrm{ij}}) \qquad (7)$$

Table 6 Confirmation experiment result

Parameter	Optical process parameters	
	Predicted	Expermental
Level	$A_3B_1C_3D_4$	$A_3B_1C_3D_4$
MRR	0.198	0.191
SR	1.425	1.465

If the factor i is controllable, the best level j*, is determined by

$$j* = \max_{\mathrm{j}}(AGV_{\mathrm{ij}}) \qquad (8)$$

3.8 Confirmation Test

Once the optimal level of the design parameters has been selected, the final step is to predict and verify the quality characteristic using the optimal level of the design parameters. Here we have used the factor levels obtained by using Eqs. 7 and 8 [26]. The estimated S/N ratio using the optimal level of the design parameters can be calculated using Eq. 9.

$$\hat{\eta} = \eta_m + \sum_{i=1}^{q} (\bar{\eta} - \eta_m) \qquad (9)$$

η_m = Average SN ratio

$\hat{\eta}$ = Average SN ratio corresponding to i_{th} significant factor on j_{th} level

q = Number of significant factors

The predicted SN ratio for the optimal setting of the parameters, that is $A_3B_1C_3D_4$ was obtained from Eq. 9 [26] is -2.45077. Table 6 shows, the both predicted and experimental results and it is evident that the experimental values are very close to predicted values. Figure 8 shows the probability plot of Grey relational grade and it evident the all the errors are within the limit for the 95% confidence level.

Table 5 Results of ANOVA on grey grade

Source	DOF	Seq SS	Adj SS	Adj MS	F	P	% Contribution
Pulse on time (Ton)	3	0.04804	0.04804	0.01601	1.06	0.481	22.02
Pulse off time (Toff)	3	0.03590	0.03590	0.01197	0.79	0.573	16.46
Wire feed (m/min)	3	0.00269	0.00269	0.00090	0.06	0.978	1.23
Peak Current (Ip)	3	0.08624	0.08624	0.02875	1.91	0.305	39.54
Error	3	0.04523	0.04523	0.01508			20.74
Total	15	0.21810					100

DOF: Degree of freedom, Seq SS: Sequential sums of squares, Adj SS: adjusted sum of squares, Adj MS: Adjusted mean squares, F: F -Test, P: Probability

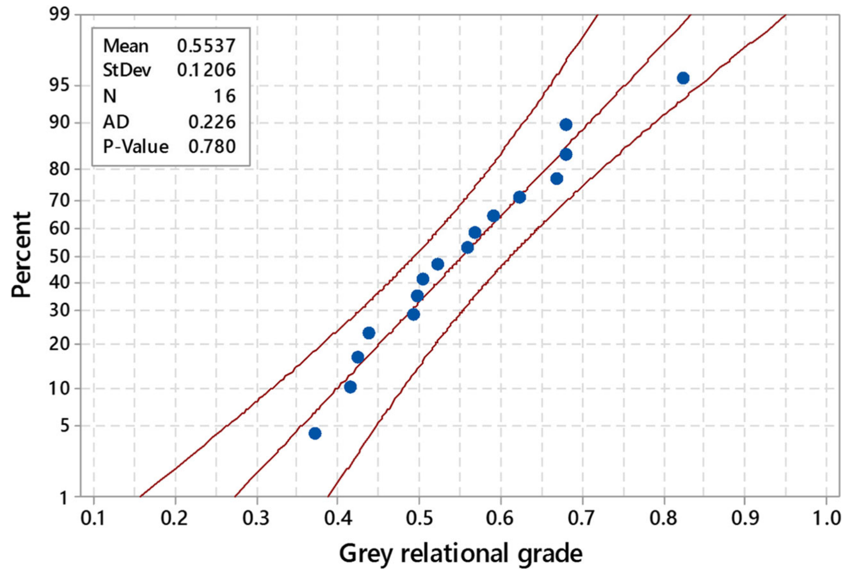

Fig. 8 Probability plot of Grey relational grade

4 Conclusions

- AA7178-10 wt. % ZrB_2 metal matrix composites were synthesized using stir casting route and their microstructure and erosion behaviour of the composites was studied.
- Grey relational analysis could be a very useful tool for predicting the Material removal rate and surface roughness of Al7178-10 wt. % ZrB_2 Stir Cast Metal Matrix Composites during WEDM machining.
- The maximum MRR and minimum SR can be achieved for the pulse on time: 112 us, pulse off time: 45 us, wire feed: 7 m/min and peak current: 11 A.
- From the ANOVA analysis, it is revealed that Peak Current and Pulse on time are prominent factors which affect the machining of Al7178-10 wt. % ZrB_2 metal matrix composites. The Peak current (39.54%) influences more on erosion of Al7178-10 wt. % ZrB_2 composite followed by Pulse on time (22.02%), Pulse off time (16.46%) and Wire feed (1.23%).

References

1. Mathan Kumar N, Senthil Kumaran S, Kumaraswamidhas LA (2015) An investigation of mechanical properties and material removal rate, tool wear rate in EDM machining process of Al2618 alloy reinforced with Si_3N_4, AlN and ZrB_2 composites. J Alloy Compd 650:318–327
2. Rengasamy NV, Rajkumar M, Senthil Kumaran S (2015) An analysis of mechanical properties and optimization of EDM process parameters of Al4032 alloy reinforced with ZrB_2 and TiB_2 in-situ composites. J Alloy Compd 662:325–338
3. Shueiwan HJ, Xue CS (2015) Investigation of mechanical properties and microstructures of aluminium fly ash composite processed by friction stirring. Mater Sci Eng A 640:314–319
4. Asadipanah Z, Rajabi M (2015) Production of Al–ZrB_2 nano-composites by microwave sintering process. J Mater Sci 26:6148–6156
5. Naveen Kumar G, Narayanasamy R, Natarajan S, Kumaresh Babu SP, Sivaprasad K, Sivasankaran S (2010) Dry sliding wear behaviour of AA 6351-ZrB_2 in situ composite at room temperature. Mater Des 31:1526–1532
6. Mckimpson MG, Scott TE (1989) Processing and properties of metal matrix composites containing discontinuous reinforcement. Mater Sci Eng A 107:93–106
7. Dinaharan I, Murugan N (2012) Dry sliding wear behavior of AA6061/ZrB2 in-situ composite. Trans Nonferrous Met Soc China 22:810–818
8. Balak Z, Zakeri M, Rahimipour M, Salahi E (2015) Taguchi design and hardness optimization of ZrB_2-based composites reinforced with chopped carbon fiber and different additives and prepared by SPS. J Alloy Compd 639:617–625
9. Balak Z, Zakeri M (2016) Application of Taguchi L32 orthogonal design to optimize flexural strength of ZrB_2-based composites prepared by spark plasma sintering. Int J Refract Met H 55:58–67
10. Thandalama SK, Ramanathan S, Sundarrajan S (2015) Synthesis microstructural and mechanical properties of ex situ zircon particles ($ZrSiO_4$) reinforced metal matrix composites (MMCs): A review. J Mater Res Technol 4:333–347
11. Abdizadeh H, Ebrahimifard R, Baghchesara MA (2014) Investigation of microstructure and mechanical properties of nano MgO reinforced Al composites manufactured by stir casting and powder metallurgy methods: A comparative study. Compos Part B-Eng 56:217–221
12. Rajan HBM, Ramabalan S, Dinaharan I, Vijay SJ (2013) Synthesis and characterization of in situ formed titanium diboride particulate reinforced AA7075 aluminum alloy cast composites. Mater Design 44:438–445
13. Ezatpour HR, Torabi-Parizi M, Sajjadi SA (2013) Microstructure and mechanical properties of extruded Al/Al_2O_3 composites fabricated by stir-casting process. Trans Nonferrous Met Soc China 23:1262–1268
14. Pozdniakov AV, Zolotorevskiy VS, Barkov RYU, Lotfy A, Bazlov AI (2016) Microstructure and material characterization of 6063/B_4C and 1545K/B_4C composites produced by two stir casting techniques for nuclear applications. J Alloy Compd 664:317–320

15. Ezatpour HR, Sajjadi SA, Sabzevar MH, Huang Y (2014) Investigation of microstructure and mechanical properties of Al6061-nanocomposite fabricated by stir casting. Mater Design 55:921–928
16. Senthilkumar V, Omprakash BU (2011) Effect of Titanium Carbide particle addition in the aluminium composite on EDM process parameters. J Manuf Process 13:60–66
17. Prasad DS, Shoba C, Varma KR, Khurshid A (2015) Influence of wire EDM parameters on the damping behaviour of A356.2 aluminum alloy. J Alloy Compd 646:257–263
18. Garg RK, Singh KK, Sachdeva A, Vishal S, Sharma KO, Singh S (2010) Review of research work in sinking EDM and WEDM on metal matrix composite materials. Int J Adv Manuf Technol 50:611–624
19. Zhang Z, Huang H, Ming W, Zhong X, Huang Y, Zhang G (2016) Study on machining characteristics of WEDM with ultrasonic vibration and magnetic field assisted techniques. J Mater Process Tech 234:342–352
20. Zhang C (2014) Effect of wire electrical discharge machining (WEDM) parameters on surface integrity of nanocomposite ceramics. Ceram Int 40:9657–9662
21. Garg RK, Singh KK, Sachdeva A, Vishal S, Sharma KO, Singh S (2010) Review of research work in sinking EDM and WEDM on metal matrix composite materials. Int J Adv Manuf Technol 50:611–624
22. Kharola A (2015) Analysis of various machining parameters of electrical discharge machining (EDM) on hard steels using copper and aluminium electrodes. IJEM 5:1–14
23. Wang A-C, Wang D-A, Chen C-C (2009) Machining performance and optimizing machining parameters of Al2O3–TiC ceramics using EDM based on the taguchi method. Mater Manuf 24:667–674
24. Kumar SS, Uthayakumar M, Kumaran ST, Parameswaran P, Mohandas E, Kempulraj G, Ramesh Babu BS, Natarajan SA (2015) Parametric optimization of wire electrical discharge machining on aluminium based composites through grey relational analysis. J Manuf Process 20:33–39
25. Manna A, Bhattacharyya B (2006) Taguchi and Gauss elimination method: A dual response approach for parametric optimization of CNC wire cut EDM of PRAlSiCMMC. Int J Adv Manuf Technol 28:67–75
26. Noorul Haq A, Marimuthu P, Jeyapaul R (2008) Multi response optimization of machining parameters of drilling Al/SiC metal matrix composite using grey relational analysis in the Taguchi method. Int J Adv Manuf Technol 37:250–255
27. Gopalakannan S, Senthilvelan T (2013) Ranganathan.S. Statistical optimization of EDM parameters on machining of aluminium hybrid metal matrix composite by applying Taguchi based grey analysis. J Sci Ind Res India 72:358–365
28. Ahilan C, Michael Rajan HB (2016) Optimization of MRR and surface roughness of in situ formed AA7075/Tib_2 composite – grey based Taguchi method. Int J Chem Sci 14:1026–1040
29. Muthuramalingam T, Mohan B (2013) Taguchi-grey based multi response optimization of electrical process parameters in electrical discharge machining. Indian J Eng Mater S 20:471–475
30. Kannan R, Kumar A, Garg MP, Singh A, Sharma N (2015) Multiple performance characteristics optimization for Al 7075 on electrical discharge drilling by Taguchi grey relational theory. J Ind Eng Int 11:459–472
31. Huang T-S, Frankel GS (2007) Kinetics of sharp intergranular corrosion fissures in AA7178. Corrosion Sci 49:858–876
32. Mondal DP, Jha N, Badkul A, Das S, Yadav MS, Jain P (2011) Effect of calcium addition on the microstructure and compressive deformation behaviour of 7178 aluminium alloy. Mater Des 32:2803–2812
33. Asadipanah Z, Rajabi M Production of Al–ZrB_2 nano-composites by microwave sintering process. J Mater Sci Mater Electron 26:6148–6156
34. Kumar NM, Kumaran SS, Kumaraswamidhas LA (2016) High temperature investigation on EDM process of Al 2618 alloy reinforced with Si_3N_4, AlN and ZrB_2 in-situ composites . J Alloy Compd 663:755–768